hep-ph/0002191

CERN-TH/2000-054
DESY 00/021

Aspects of GMSB Phenomenology at TeV Colliders

Report of the GMSB SUSY Working Group
Workshop "Physics at TeV Colliders"
Les Houches, 7-18 June 1999

S. Ambrosanio [a,⋆] (convener), **S. Heinemeyer** [b], **B. Mele** [c], **S. Petrarca** [c], **G. Polesello** [d], **A. Rimoldi** [d,e], **G. Weiglein** [a]

[a] CERN – *Theory Division, CH-1211 Geneva 23, Switzerland*

[b] DESY – *Theory Group, Notkestr. 85, D-22603 Hamburg, Germany*

[c] INFN – *Sezione di Roma I e Dipartimento di Fisica, Università "La Sapienza", p. le Aldo Moro 2, I-00185 Roma, Italy*

[d] INFN – *Sezione di Pavia e Dip. Fis. Nucl. Teor., Università di Pavia, via Bassi 6, I-27100 Pavia, Italy*

[e] CERN – *EP Division, CH-1211 Geneva 23, Switzerland*

Abstract

The status of two on-going studies concerning important aspects of the phenomenology of gauge-mediated supersymmetry breaking (GMSB) models at TeV colliders is reported.
The first study deals with the characteristics of the light Higgs boson spectrum allowed by the (minimal and non-minimal) GMSB framework. Today's most accurate GMSB model generation and two-loop Feynman-diagrammatic calculation of m_h have been combined. The Higgs masses are shown in dependence of various model parameters at the messenger and electroweak scales. In the minimal model, an upper limit on m_h of about 124 GeV is found for $m_t = 175$ GeV.
The second study is focused on the measurement of the fundamental SUSY breaking scale $\sqrt{F}$ at the LHC in the GMSB scenario where a stau is the next-to-lightest SUSY particle (NLSP) and decays into a gravitino with $c\tau_{\rm NLSP}$ in the range 0.5 m to 1 km. This implies the measurement of mass and lifetime of long lived sleptons. The identification is performed by determining the time of flight in the ATLAS muon chambers. Accessible range and precision on $\sqrt{F}$ achievable with a counting method are assessed.

⋆ E-mail: ambros@mail.cern.ch

1 Introduction to Gauge-Mediated SUSY Breaking

Since no superpartners have been detected at collider experiments so far, supersymmetry (SUSY) cannot be an exact symmetry of Nature. The requirement of "soft" supersymmetry breaking [1] alone is not sufficient to reduce the free parameters to a number suitable for predictive phenomenological studies. Hence, motivated theoretical hypotheses on the nature of SUSY breaking and the mechanism through which it is transmitted to the visible sector of the theory [here assumed to be the one predicted by the minimal SUSY extension of the standard model (MSSM)] are highly desirable. If SUSY is broken at energies of the order of the Planck mass and the SUSY breaking sector communicates with the MSSM sector through gravitational interactions only, one falls in the supergravity-inspired (SUGRA) scheme. The most recognised alternative to SUGRA is based instead on the hypothesis that SUSY breaking occurs at relatively low energy scales and it is mediated mainly by gauge interactions (GMSB) [2–4]. A good theoretical reason to consider such a possibility is that it provides a natural, automatic suppression of the SUSY contributions to flavour-changing neutral current and $\mathcal{CP}$-violating processes. A pleasant consequence is that, at least in the simplest versions of GMSB, the MSSM spectrum and other observables depend on just a handful of parameters, typically

$$M_{\rm mess},\ N_{\rm mess},\ \Lambda,\ \tan\beta,\ {\rm sign}(\mu), \tag{1}$$

where $M_{\rm mess}$ is the overall messenger scale; $N_{\rm mess}$ is the so-called messenger index, parameterising the structure of the messenger sector; Λ is the universal soft SUSY breaking scale felt by the low-energy sector; $\tan\beta$ is the ratio of the vacuum expectation values of the two Higgs doublets; sign(μ) is the ambiguity left for the SUSY higgsino mass after conditions for correct electroweak symmetry breaking (EWSB) are imposed (see e.g. Refs. [5–8]).

The phenomenology of GMSB (and more in general of any theory with low-energy SUSY breaking) is characterised by the presence of a very light gravitino $\tilde{G}$ [9],

$$m_{3/2} \equiv m_{\tilde{G}} = \frac{F}{\sqrt{3}M'_P} \simeq \left(\frac{\sqrt{F}}{100\ {\rm TeV}}\right)^2 2.37\ {\rm eV}, \tag{2}$$

where $\sqrt{F}$ is the fundamental scale of SUSY breaking, 100 TeV is a typical value for it, and $M'_P = 2.44 \times 10^{18}$ GeV is the reduced Planck mass. Hence, the $\tilde{G}$ is always the lightest SUSY particle (LSP) in these theories. If R-parity is assumed to be conserved, any produced MSSM particle will finally decay into the gravitino. Depending on $\sqrt{F}$, the interactions of the gravitino, although much weaker than gauge and Yukawa interactions, can still be strong enough to be of relevance for collider physics. As a result, in most cases the last step of any SUSY decay chain is the decay of the next-to-lightest SUSY particle (NLSP), which can occur outside or inside a typical detector or even close to the interaction point. The pattern of the resulting spectacular signatures is determined by the identity of the NLSP and its lifetime before decaying into the $\tilde{G}$,

$$c\tau_{\rm NLSP} \simeq \frac{1}{100\mathcal{B}}\left(\frac{\sqrt{F}}{100\ {\rm TeV}}\right)^4 \left(\frac{m_{\rm NLSP}}{100\ {\rm GeV}}\right)^{-5}, \tag{3}$$

where $\mathcal{B}$ is a number of order unity depending on the nature of the NLSP.

The identity of the NLSP [or, to be more precise, the identity of the sparticle(s) having a large branching ratio (BR) for decaying into the gravitino and the relevant SM partner] determines four main scenarios giving rise to qualitatively different phenomenology:

Neutralino NLSP scenario: Occurs whenever $m_{\tilde{N}_1} < (m_{\tilde{\tau}_1} - m_\tau)$. Here typically a decay of the $\tilde{N}_1$ to $\tilde{G}\gamma$ is the final step of decay chains following any SUSY production process. As a consequence, the main inclusive signature at colliders is prompt or displaced photon pairs + X + missing energy. $\tilde{N}_1$ decays to $\tilde{G}Z^0$ and other minor channels may also be relevant at TeV colliders.

Stau NLSP scenario: Defined by $m_{\tilde{\tau}_1} < \mathrm{Min}[m_{\tilde{N}_1}, m_{\tilde{\ell}_R}] - m_\tau$, features $\tilde{\tau}_1 \to \tilde{G}\tau$ decays, producing τ pairs or charged semi-stable $\tilde{\tau}_1$ tracks or decay kinks + X + missing energy. Here and in the following, ℓ stands for e or μ.

Slepton co-NLSP scenario: When $m_{\tilde{\ell}_R} < \mathrm{Min}[m_{\tilde{N}_1}, m_{\tilde{\tau}_1} + m_\tau]$, $\tilde{\ell}_R \to \tilde{G}\ell$ decays are also open with large BR. In addition to the signatures of the stau NLSP scenario, one also gets $\ell^+\ell^-$ pairs or $\tilde{\ell}_R$ tracks or decay kinks.

Neutralino-stau co-NLSP scenario: If $|m_{\tilde{\tau}_1} - m_{\tilde{N}_1}| < m_\tau$ and $m_{\tilde{N}_1} < m_{\tilde{\ell}_R}$, both signatures of the neutralino NLSP and stau NLSP scenario are present at the same time, since $\tilde{N}_1 \leftrightarrow \tilde{\tau}_1$ decays are not allowed by phase space.

Note that in the GMSB parameter space the relation $m_{\tilde{\ell}_R} > m_{\tilde{\tau}_1}$ always holds. Also, one should keep in mind that the classification above is only valid as an indicative scheme in the limit m_e, $m_\mu \to 0$, neglecting also those cases where a fine-tuned choice of $\sqrt{F}$ and the sparticle masses may give rise to competition between phase-space suppressed decay channels from one ordinary sparticle to another and sparticle decays to the gravitino [10].

In this report, we treat two important aspects of the GMSB phenomenology at TeV colliders:

(A) The consequences of the GMSB hypotheses on the light Higgs spectrum using the most accurate tools available today for model generation and m_h calculation;

(B) Studies and possible measurements at the LHC with the ATLAS detector in the stau NLSP or slepton co-NLSP scenarios, with focus on determining the fundamental SUSY breaking scale $\sqrt{F}$.

For this purpose, we generated about 30000 GMSB models under well defined hypotheses, using the program `SUSYFIRE` [11], as described in the following section.

2 GMSB Models

In the GMSB framework, the pattern of the MSSM spectrum is simple, as all sparticle masses are generated in the same way and scale approximately with a single parameter Λ, which sets the amount of soft SUSY breaking felt by the visible sector. As a consequence, scalar and gaugino masses are related to each other at a high energy scale, which is not the case in other SUSY frameworks, e.g. SUGRA. Also, it is possible to impose other conditions at a lower scale to achieve EWSB and further reduce the dimension of the parameter space.

To build our GMSB models, we adopt the usual phenomenological approach, in particular following Ref. [8], where problems relevant for GMSB physics at TeV colliders were also approached. We do not specify the origin of the SUSY higgsino mass μ, nor do we assume that the analogous soft SUSY breaking parameter $B\mu$ vanishes at the messenger scale. Instead, we impose correct EWSB to trade μ and $B\mu$ for M_Z and $\tan\beta$, leaving the

sign of μ undetermined. However, we are aware that to build a satisfactory GMSB model one should also solve the latter problem in a more fundamental way, perhaps by providing a dynamical mechanism to generate μ and $B\mu$, possibly with values of the same order of magnitude. This might be accomplished radiatively through some new interactions. However, in this case the other soft terms in the Higgs potential, namely $m^2_{H_{1,2}}$, will be also affected and this will in turn change the values of $|\mu|$ and $B\mu$ coming from EWSB conditions [4–6]. Within the study **(A)**, we are currently considering some "non-minimal" possibilities for GMSB models that to some extent take this problem into account, and we are trying to assess the impact on the light Higgs mass. We do not treat this topic here, but refer to [12] for further details.

To determine the MSSM spectrum and low-energy parameters, we solve the renormalisation group equation (RGE) evolution with the following boundary conditions at the $M_{\rm mess}$ scale,

$$\begin{aligned} M_a &= N_{\rm mess}\Lambda g\left(\frac{\Lambda}{M_{\rm mess}}\right)\frac{\alpha_a}{4\pi}, \quad (a=1,2,3) \\ \tilde{m}^2 &= 2N_{\rm mess}\Lambda^2 f\left(\frac{\Lambda}{M_{\rm mess}}\right)\sum_a\left(\frac{\alpha_a}{4\pi}\right)^2 C_a, \end{aligned} \tag{4}$$

respectively for the gaugino and the scalar masses. In Eq. (4), g and f are the one-loop and two-loop functions whose exact expressions can be found e.g. in Ref. [7], and C_a are the quadratic Casimir invariants for the scalar fields. As usual, the scalar trilinear couplings A_f are assumed to vanish at the messenger scale, as suggested by the fact that they (and not their squares) are generated via gauge interactions with the messenger fields at the two loop-level only.

To single out the interesting region of the GMSB parameter space, we proceed as follows. Barring the case where a neutralino is the NLSP and decays outside the detector (large $\sqrt{F}$), the GMSB signatures are very spectacular and are generally free from SM background. Keeping this in mind and being interested in GMSB phenomenology at future TeV colliders, we consider only models where the NLSP mass is larger than 100 GeV, assuming that searches at LEP and Tevatron, if unsuccessful, will in the end exclude a softer spectrum in most cases. We require that $M_{\rm mess} > 1.01\Lambda$, to prevent an excess of fine-tuning of the messenger masses, and that the mass of the lightest messenger scalar be at least 10 TeV. We also impose $M_{\rm mess} > M_{\rm GUT}\,\exp(-125/N_{\rm mess})$, to ensure perturbativity of gauge interactions up to the GUT scale. Further, we do not consider models with $M_{\rm mess} \gtrsim 10^5\Lambda$. As a result of this and other constraints, the messenger index $N_{\rm mess}$, which we assume to be an integer independent of the gauge group, cannot be larger than 8. To prevent the top Yukawa coupling from blowing up below the GUT scale, we require $\tan\beta > 1.2$ (and in some cases > 1.5). This is also motivated by the current bounds from SUSY Higgs searches at LEP II [13]. Models with $\tan\beta \gtrsim 55$ (with a mild dependence on Λ) are forbidden by the EWSB requirement and typically fail in giving $m_A^2 > 0$.

To calculate the NLSP lifetime relevant to our study **(B)**, one needs to specify the value of the fundamental SUSY breaking scale $\sqrt{F}$ on a model-by-model basis. Using perturbativity arguments, for each given set of GMSB parameters, it is possible to determine a lower bound according to Ref. [7],

$$\sqrt{F} \geq \sqrt{F_{\rm mess}} \equiv \sqrt{\Lambda M_{\rm mess}} > \Lambda. \tag{5}$$

On the contrary, no solid arguments can be used to set an upper limit on $\sqrt{F}$ of relevance for collider physics, although some semi-qualitative cosmological arguments are sometimes evoked.

To generate our model samples using `SUSYFIRE`, we used logarithmic steps for Λ (between about 45 TeV/$N_{\rm mess}$ and about 220 TeV/$\sqrt{N_{\rm mess}}$, which corresponds to excluding models with sparticle masses above ~ 4 TeV), $M_{\rm mess}/\Lambda$ (between 1.01 and 10^5) and $\tan\beta$ (between 1.2 and about 60), subject to the constraints described above. `SUSYFIRE` starts from the values of SM particle masses and gauge couplings at the weak scale and then evolves up to the messenger scale through RGE's. At the messenger scale, it imposes the boundary conditions (4) for the soft sparticle masses and then evolves the full set of RGE's back to the weak scale. The decoupling of each sparticle at the proper threshold is taken into account. Two-loop RGE's are used for gauge couplings, third generation Yukawa couplings and gaugino soft masses. The other RGE's are taken at the one-loop level. At the scale $\sqrt{m_{\tilde{t}_1} m_{\tilde{t}_2}}$, EWSB conditions are imposed by means of the one-loop effective potential approach, including corrections from stops, sbottoms and staus. The program then evolves up again to $M_{\rm mess}$ and so on. Three or four iterations are usually enough to get a good approximation for the MSSM spectrum.

(A) The Light Higgs Boson Spectrum in GMSB Models

Contribution by:
S. Ambrosanio, S. Heinemeyer, G. Weiglein

A.1 Introduction

Within the MSSM, the masses of the $\mathcal{CP}$-even neutral Higgs bosons are calculable in terms of the other low-energy parameters. The mass of the lightest Higgs boson, m_h, has been of particular interest, as it is bounded to be smaller than the Z^0 boson mass at the tree level. The one-loop results [14–17] for m_h have been supplemented in the last years with the leading two-loop corrections, performed in the renormalisation group (RG) approach [18, 19], in the effective potential approach [20] and most recently in the Feynman-diagrammatic (FD) approach [21–23]. The two-loop corrections have turned out to be sizeable. They can lower the one-loop results by up to 20%. These calculations predict an upper bound on m_h of about $m_h \leq 130$ GeV for an unconstrained MSSM with $m_t = 175$ GeV and a common SUSY mass scale $M_{\rm SUSY} \leq 1$ TeV.

As discussed in Sec. 1, the GMSB scenario provides a relatively simple set of constraints and thus constitutes a very predictive and readily testable realization of the MSSM. The main goal of the present analysis is to study the spectrum of the lightest neutral $\mathcal{CP}$-even Higgs boson, m_h, within the GMSB framework. Particular emphasis is given to the maximal value of m_h achievable in GMSB after an exhaustive scanning of the parameter space. Our results are discussed in terms of the GMSB constraints on the low-energy parameters and compared to the cases of a SUGRA-inspired or an unconstrained MSSM.

A.2 Calculation of m_h

To evaluate m_h, we employ the currently most accurate calculation based on the FD approach [21–23]. The most important radiative corrections to m_h arise from the top and scalar top sector of the MSSM, with the input parameters m_t, the masses of the scalar top quarks, $m_{\tilde{t}_1}$, $m_{\tilde{t}_2}$, and the $\tilde{t}$-mixing angle, $\theta_{\tilde{t}}$. Here we adopt the conventions introduced in Ref. [22]. The complete diagrammatic one-loop result [16] has been combined with the dominant two-loop corrections of $\mathcal{O}(\alpha\alpha_s)$ [21, 22] and with the subdominant corrections of $\mathcal{O}(G_F^2 m_t^6)$ [18,19]. GMSB models are generated with the program `SUSYFIRE`, according to the discussion of Sec. 2. For this study, we consider only models with $\tan\beta > 1.5$ [13] and $m_A > 80$ GeV [24]. In addition, we always use $m_t = 175$ GeV. A change of 1 GeV in m_t translates roughly into a shift of 1 GeV (with the same sign) in m_h as well. Thus, changing m_t affects our results on m_h in an easily predictable way.

The results of the m_h calculation have been implemented in the program `FeynHiggs` [25]. This `Fortran` code has been combined with `SUSYFIRE`, which has been used to calculate the low energy parameters $m_{\tilde{t}_1}$, $m_{\tilde{t}_2}$, $\theta_{\tilde{t}}$, μ, M_1, M_2, $m_{\tilde{g}}$, ... for each of the ∼30000 GMSB models generated. These have then been passed to `FeynHiggs` for the m_h evaluation in a coherent way. Indeed, we transform the $\overline{\rm MS}$ parameters in the `SUSYFIRE` output into on-shell parameters before feeding them into `FeynHiggs`. Compact expressions for the relevant transition formulas can be found in Refs. [26, 27].

Compared to an existing analysis in the GMSB framework [28], we use a more complete evaluation of m_h. This leads in particular to smaller values of m_h for a given set of input parameters in our analysis. Also, in Ref. [28] although some GMSB scenarios with generalised messenger sectors were considered, the parameter space for the "minimal" case with a unique, integer messenger index $N_{\rm mess} = N_1 = N_2 = N_3$ was not fully explored. Indeed, Λ was in most cases limited to values smaller than 100 TeV and $M_{\rm mess}$ was fixed to 10^5 TeV. Furthermore, partly as a consequence of the above assumptions, the authors did not consider models with $N_{\rm mess} > 4$, i.e. their requirements for perturbativity of the MSSM gauge couplings up to the GUT scale were stronger than ours. We will see in the following section that maximal m_h values in our analysis are instead obtained for larger values of the messenger scale and the messenger index.

A.3 The Light Higgs Spectrum in GMSB

In the following, we give some results in the form of scatter plots showing the pattern in GMSB for m_h, m_A as well as other low-energy parameters of relevance for the light Higgs spectrum.

In Fig. 1(a), we show the dependence of m_h on $\tan\beta$, where only models with $\tan\beta > 1.5$, $m_A > 80$ GeV and $m_{\rm NLSP} > 100$ GeV are considered, while m_t is fixed to 175 GeV. The dependence is strong for small $\tan\beta \lesssim 10$, while for larger $\tan\beta$ the increase of the lightest Higgs mass is rather mild. The maximum values for $m_h \simeq 124$ GeV are achieved for $\tan\beta > 50$. It should be noted that for very large $\tan\beta \gtrsim 52$, we also find a few models with relatively small $m_h \lesssim 100$ GeV. This is due to the fact that in this case EWSB conditions tend to drive m_A toward very small values (cfr. Sec. 2). This is made visible by the scatter plot in Fig. 1(b), where the pseudoscalar Higgs mass is shown as a function of $\tan\beta$. For such small values of m_A and for large $\tan\beta$, the relation $m_h \approx m_A$ holds. Thus small m_h values are quite natural in this region of the parameter space. On the other hand, one can see that extremely large values of $m_A \gtrsim 2$ TeV can only be

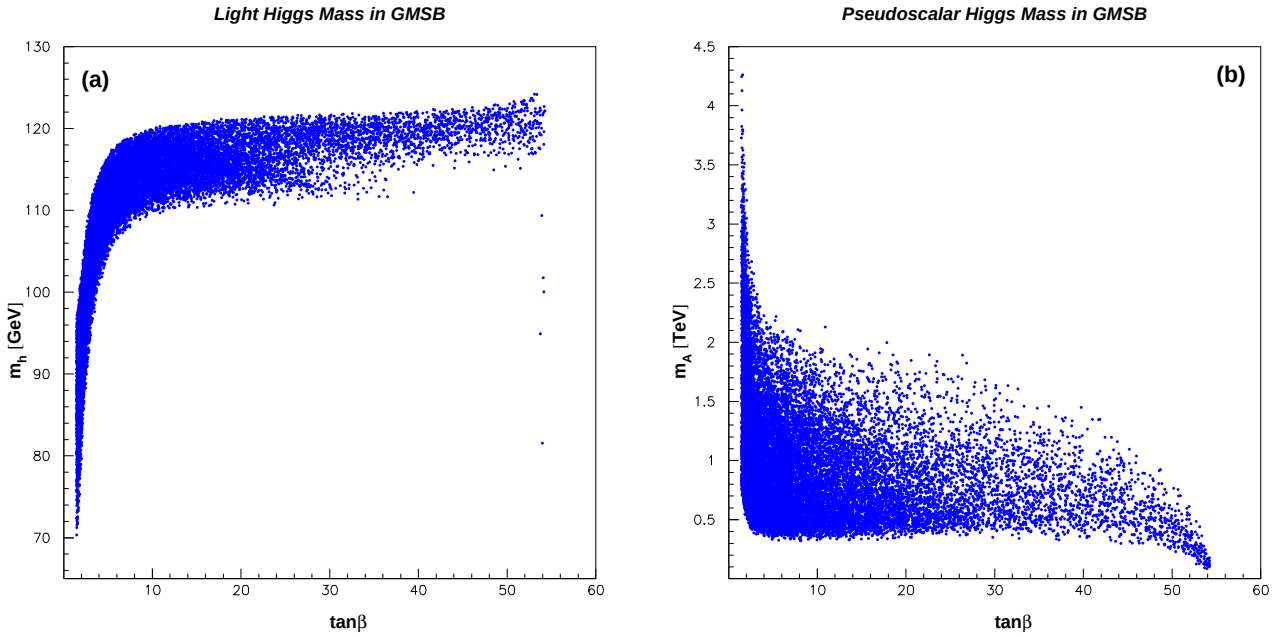

Figure 1: *Scatter plots for the light scalar (a) and pseudoscalar (b) Higgs masses as functions of* $\tan\beta$. *Only GMSB models with* $\tan\beta > 1.5$, $m_A > 80$ *GeV and* $m_{\rm NLSP} > 100$ *GeV are considered.*

obtained for small or moderate $\tan\beta \lesssim 10$ GeV. A comparison between Fig 1(a) and (b) reveals that the largest m_h values $\gtrsim 123$ GeV correspond in GMSB to m_A values in the 300–800 GeV range. Indeed, it has been checked that such large m_h values are in general obtained in the FD calculation for $300 \lesssim m_A \lesssim 1000$ GeV, see Ref. [22].

In Fig. 2, we show the dependence of the lightest Higgs boson mass on the stop mixing parameter $x_{\rm top}$ defined by

$$x_{\rm top} \equiv \frac{A_{\rm top} - \mu/\tan\beta}{m_S}, \quad \text{where} \quad m_S = \sqrt{(m_{\tilde{t}_1}^2 + m_{\tilde{t}_2}^2)/2}. \tag{6}$$

For equal soft SUSY breaking parameters in the stop sector with the D-terms neglected, $x_{\rm top}$ corresponds to the ratio X_t/M_S of the off-diagonal and diagonal entries in the stop mixing matrix, see e.g. Ref. [27].

Maximal m_h values are obtained for $x_{\rm top} \approx \pm 2$, a minimum is reached around $x_{\rm top} \approx 0$. Thus, for large m_h values a large numerator in Eq. (6) is required. From Fig. 3(a), one can see that in GMSB only negative values of $A_{\rm top}$ are allowed at the electroweak scale, as a consequence of the fact that the trilinear couplings are negligible at the messenger scale. Due to the logarithmic dependence of m_h on the stop masses, relatively large values of $|A_{\rm top}|$ are needed for large m_h. In addition, large $\tan\beta$ is also required. From Fig. 3(b) one can check that this leads to values of $x_{\rm top} \approx -0.95$, which can only be achieved for positive μ. Fig. 4(a) shows the dependence of $A_{\rm top}$ on μ. Large values of $|A_{\rm top}|$ are only reached for large $|\mu|$ values. Therefore maximal h masses are obtained for relatively large and positive μ, as can be seen in Fig. 4(b).[1]

[1] In general, for large values of $|\mu|$ and $\tan\beta$ the effects of the corrections from the b–$\tilde{b}$ sector can become important, leading to a decrease in m_h. For the GMSB models under consideration, however, this is not the case as a consequence of the relatively large $\tilde{b}$ masses.

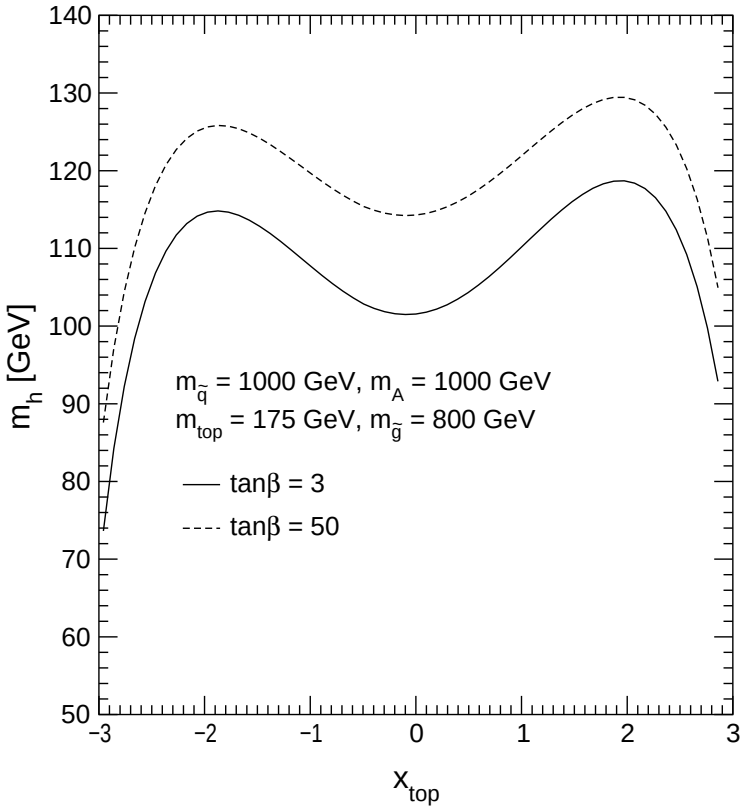

Figure 2: *The light $\mathcal{CP}$-even Higgs boson mass is given as a function of $x_{\rm top}$ for $\tan\beta = 3, 50$, $m_A = 1000$ GeV, a common soft SUSY breaking scale for the squarks, $m_{\tilde{q}} = 1000$ GeV, and a gluino mass $m_{\tilde{g}} = 800$ GeV.*

All these arguments about the combination of low energy parameters needed for large m_h in GMSB are summarised in Tab. 1, where we report the 10 models in our sample that give rise to the highest m_h values. Together with m_h, Tab. 1 shows the corresponding input GMSB parameters [cfr. Eq. (1)] as well as the values of the low energy parameters mentioned above.

It is interesting to note that all the models shown in Tab. 1 feature a large messenger index and values of the messenger scale not far from the maximum we allowed while generating GMSB models. We could not construct a single model with $m_h \gtrsim 122.5$ GeV having $N_{\rm mess} < 6$ or $M_{\rm mess} < 10^5$ TeV, for $m_t = 175$ GeV. It is hence worth mentioning here that our choice of imposing $M_{\rm mess}/\Lambda < 10^5 \Rightarrow M_{\rm mess} \lesssim 2 \times 10^{10}$ GeV does not correspond to any solid theoretical prejudice. On the other hand it is true that $M_{\rm mess} \gtrsim 3 \times 10^8$ GeV always corresponds to gravitino masses larger than ~ 1 keV, due to Eqs. (2) and (5). The latter circumstance might be disfavoured by cosmological arguments [29]. A curious consequence is that the GMSB models with the highest m_h belong always to the stau NLSP or slepton co-NLSP scenarios.

Note also that restricting ourselves to GMSB models with $\Lambda < 100$ TeV, $M_{\rm mess} < 10^5$ TeV and $N_{\rm mess} \leq 4$, we find a maximal m_h value of 122.2 GeV, for $m_t = 175$ GeV and $\tan\beta \sim 52$. This is to be compared with the one-loop result of Ref. [28], $m_h(\max) = 131.7$, for $\tan\beta$ around 30 (the assumed value of m_t is not quoted).

Values for m_h slightly larger than those we found here may also arise from non-minimal contributions to the Higgs potential, in connection with a dynamical generation of μ and $B\mu$ (cfr. Sec. 2). A treatment of this problem can be found in Ref. [12].

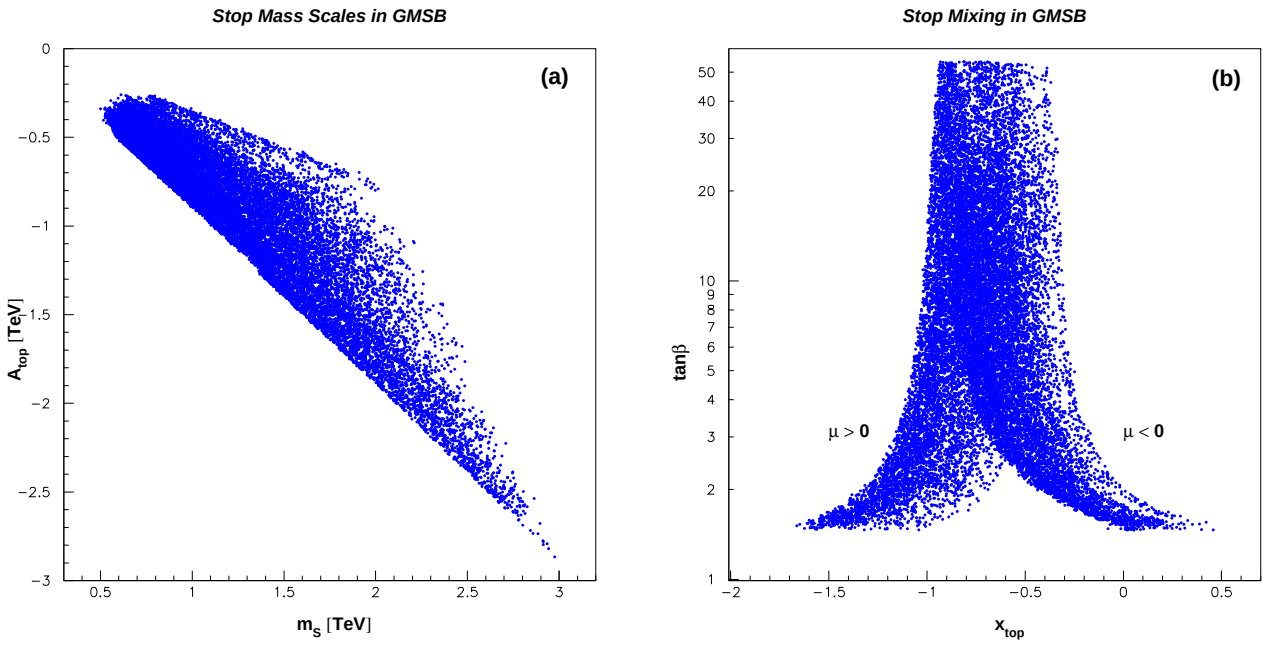

Figure 3: *Scatter plots of* $A_{\rm top}$ *vs.* m_S*, the mass scale appearing in the denominator of Eq. (6) (a) and* $\tan\beta$ *vs.* $x_{\rm top}$ *(b).*

One should also keep in mind that our analysis still suffers from uncertainties due to unknown higher order corrections both in the RGE's for GMSB model generation and in the evaluation of m_h from low energy parameters. A rough estimate of these effects leads to shifts in m_h not larger than 3 to 5 GeV.

A.4 Conclusions

We conclude that in the minimal GMSB framework described above, values of $m_h \gtrsim 124.2$ GeV are not allowed for $m_t = 175$ GeV. This is almost 6 GeV smaller than the maximum value for m_h one can achieve in the MSSM without any constraints or assumptions about the structure of the theory at high energy scales [22, 30, 31]. On the other hand, the alternative mSUGRA framework allows values of m_h that are ~ 3 GeV larger than in GMSB [13]. This makes the GMSB scenario slightly easier to explore via Higgs boson search. This result was expected in the light of the rather strong GMSB requirements, such as the presence of a unique soft SUSY breaking scale, the relative heaviness of the squarks and the gluino compared to non-strongly interacting sparticles, and the fact that the soft SUSY breaking trilinear couplings A_f get nonzero values at the electroweak scale only by RGE evolution. Nevertheless, once the whole parameter space is explored, it is not true that mGMSB gives rise to m_h values that are considerably smaller than in mSUGRA. Even smaller differences in the maximal m_h might be present when considering non-minimal, complex messenger sectors [28] or additional contributions to the Higgs potential [5, 12]. In any case, as for mSUGRA, current LEP II or Tevatron data on Higgs boson searches are far from excluding mGMSB, and the upgraded Tevatron and the LHC will certainly be needed to deeply test any realistic SUSY model.

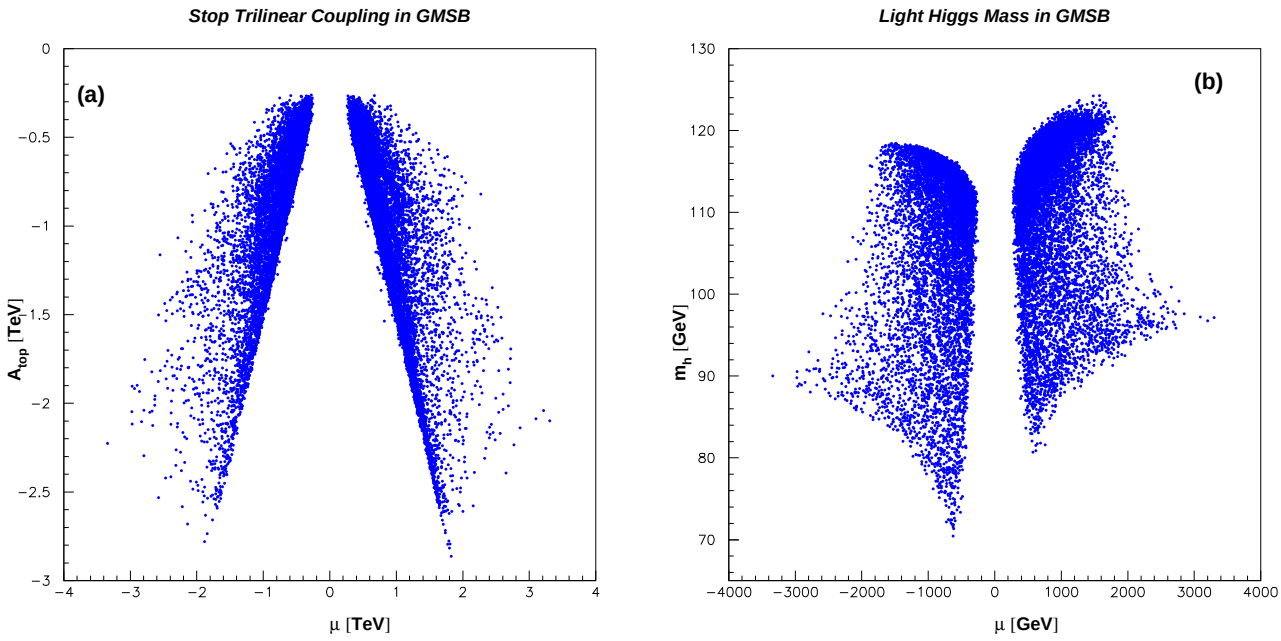

Figure 4: *Scatter plots for $A_{\rm top}$ (a) and the light scalar Higgs mass (b) vs. the SUSY higgsino mass μ evaluated at the electroweak scale.*

ID	m_h GeV	$N_{\rm mess}$	$M_{\rm mess}$ 10^6 TeV	Λ TeV	μ GeV	$\tan\beta$	m_A GeV	$m_{\tilde{t}_1}$ GeV	$m_{\tilde{t}_2}$ GeV	$A_{\rm top}$ GeV	$x_{\rm top}$
A1	124.2	7	1.00	72.7	1470	53.4	367	2320	2510	-2150	-0.90
A2	124.2	8	4.48	66.7	1570	53.1	436	2400	2600	-2310	-0.94
A3	123.7	6	2.07	87.0	1580	52.8	485	2420	2630	-2240	-0.90
A4	123.7	8	4.67	52.4	1270	52.9	373	1930	2100	-1850	-0.93
A5	123.5	8	4.89	51.1	1250	52.7	388	1880	2050	-1810	-0.93
A6	123.5	6	2.54	67.1	1260	53.0	349	1910	2080	-1760	-0.89
A7	123.4	8	4.62	61.6	1470	51.9	549	2230	2430	-2160	-0.94
A8	123.4	6	4.15	88.1	1630	51.9	609	2450	2670	-2300	-0.91
A9	123.3	7	3.77	70.3	1490	51.8	567	2260	2460	-2150	-0.92
A10	123.3	8	3.74	72.1	1677	50.7	756	2580	2800	-2500	-0.94

Table 1: *The 10 GMSB models giving rise to the highest m_h values in our sample. For each model, together with the light Higgs mass, we show the values of the GMSB input parameters and other low energy parameters of interest for calculating m_h.*

Acknowledgements

S. A. and S. H. thank the organisers of the Workshop "Physics at TeV Colliders", for the hospitality and the pleasant and productive atmosphere in Les Houches.

(B) Measuring the SUSY Breaking Scale at the LHC in the Slepton NLSP Scenario of GMSB Models

Contribution by:
S. Ambrosanio, B. Mele, S. Petrarca, G. Polesello, A. Rimoldi

B.1 Introduction

The fundamental scale of SUSY breaking $\sqrt{F}$ is perhaps the most important quantity to determine from phenomenology in a SUSY theory. In the mSUGRA framework, the gravitino mass sets the scale of the soft SUSY breaking masses in the MSSM ($\sim 0.1 - 1$ TeV), so that $\sqrt{F}$ is typically large $\sim 10^{10-11}$ GeV [cfr. Eq. (2)]. As a consequence, the interactions of the $\tilde{G}$ with the other MSSM particles $\sim F^{-1}$ are too weak for the gravitino to be of relevance in collider physics and there is no direct way to access $\sqrt{F}$ experimentally. In GMSB theories, the situation is completely different. The soft SUSY breaking scale of the MSSM and the sparticle masses are set by gauge interactions between the messenger and low energy sectors to be $\sim \alpha_{\rm SM}\Lambda$ [cfr. Eq. (4)], so that typical Λ values are $\sim 10 - 100$ TeV. On the other hand, $\sqrt{F}$ is subject to the lower bound (5) only, which tells us that values well below 10^{10} GeV and even as low as several tens of TeV are perfectly reasonable. The $\tilde{G}$ is in this case the LSP and its interactions are strong enough to allow NLSP decays to the $\tilde{G}$ inside a typical detector size. The latter circumstance gives us a chance for extracting $\sqrt{F}$ experimentally through a measurement of the NLSP mass and lifetime [cfr. Eq. (3)].

Furthermore, the possibility of determining $\sqrt{F}$ with good precision opens a window on the physics of the SUSY breaking (the so-called "secluded") sector and the way this SUSY breaking is transmitted to the messenger sector. Indeed, the characteristic scale of SUSY breaking felt by the messengers (and hence the MSSM sector) given by $\sqrt{F_{\rm mess}}$ in Eq. (5) can be also determined once the MSSM spectrum is known. By comparing the measured values of $\sqrt{F}$ and $\sqrt{F_{\rm mess}}$ it might well be possible to get information on the way the secluded and messenger sector communicate to each other. For instance, if it turns out that $\sqrt{F_{\rm mess}} \ll \sqrt{F}$, then it is very likely that the communication occurs radiatively and the ratio $\sqrt{F_{\rm mess}/F}$ is given by some loop factor. On the contrary, if the communication occurs via a direct interaction, this ratio is just given by a Yukawa-type coupling constant, with values $\lesssim 1$, see Refs. [4, 7].

An experimental method to determine $\sqrt{F}$ at a TeV scale e^+e^- collider through the measurement of the NLSP mass and lifetime was presented in Ref. [8], in the neutralino NLSP scenario. Here, we are concerned about the same problem, but at a hadron collider, the LHC, and in the stau NLSP or slepton co-NLSP scenarios. These scenarios provide a great opportunity at the LHC, since the characteristic signatures with semi-stable charged tracks are muon-like, but come from massive sleptons with a β significantly smaller than 1. In particular, we perform our simulations in the ATLAS muon detector, whose large size and excellent time resolution [32] allow a precision measurement of the slepton time of flight from the production vertex out to the muon chambers and hence of the slepton velocity. Moreover, in the stau NLSP or slepton co-NLSP scenarios, the knowledge of the

ID	$M_{\rm mess}$ (TeV)	$N_{\rm mess}$	Λ (TeV)	$\tan\beta$	sign(μ)
B1	1.79×10^4	3	26.6	7.22	–
B2	5.28×10^4	3	26.0	2.28	–
B3	4.36×10^2	5	41.9	53.7	+
B4	1.51×10^2	4	28.3	1.27	–
B5	3.88×10^4	6	58.6	41.9	+
B6	2.31×10^5	3	65.2	1.83	–
B7	7.57×10^5	3	104	8.54	–
B8	4.79×10^2	5	71.9	3.27	–

Table 2: *Input parameters of the sample GMSB models chosen for our study.*

NLSP mass and lifetime is sufficient to determine $\sqrt{F}$, since the factor $\mathcal{B}$ in Eq. (3) is exactly equal to 1. This is not the case in the neutralino NLSP scenario, where $\mathcal{B}$ depends at least on the neutralino physical composition, and more information and measurements are needed for extracting a precise value of $\sqrt{F}$.

B.2 Choice of the Sample Models and Event Simulation

The two main parameters affecting the experimental measurement at the LHC of the slepton NLSP properties are the slepton mass and momentum distribution. Indeed, at a hadron collider most of the NLSP's come from squark and gluino production, followed by cascade decays. Thus, the momentum distribution is in general a function of the whole MSSM spectrum. However, one can approximately assume that most of the information on the NLSP momentum distribution is provided by the squark mass scale $m_{\tilde{q}}$ only (in the stau NLSP scenario or slepton co-NLSP scenarios of GMSB, one generally finds $m_{\tilde{g}} \gtrsim m_{\tilde{q}}$). To perform detailed simulations, we select a representative set of GMSB models generated by `SUSYFIRE`. We limit ourselves to models with $m_{\rm NLSP} > 100$ GeV, motivated by the discussion in Sec. 2, and $m_{\tilde{q}} < 2$ TeV, in order to yield an adequate event statistics after a three-year low-luminosity run (corresponding to 30 fb^{-1}) at the LHC. Within these ranges, we choose eight extreme points (four in the stau NLSP scenario and four in the slepton co-NLSP scenario) allowed by GMSB in the ($m_{\rm NLSP}$, $m_{\tilde{q}}$) plane, in order to cover the various possibilities.

In Tab. 2, we list the input GMSB parameters we used to generate these eight points, while in Tab. 3 we report the corresponding values of the stau mass, the squark mass scale and the gluino mass. The "NLSP" column indicates whether the model belongs to the stau NLSP or slepton co-NLSP scenario. The last column gives the total cross section in pb for producing any pairs of SUSY particles at the LHC.

For each model, the events were generated with the `ISAJET` Monte Carlo [33] that incorporates the calculation of the SUSY mass spectrum and branching fraction using the GMSB parameters as input. We have checked that for the eight model points considered the sparticle masses calculated with `ISAJET` are in good agreement with the output of `SUSYFIRE`.

The generated events were then passed through `ATLFAST` [34], a fast particle-level simulation of the ATLAS detector. The `ATLFAST` package, however, was only used to evaluate the efficiency of the calorimetric trigger that selects the GMSB events. The

ID	$m_{\tilde{\tau}_1}$ (GeV)	"NLSP"	$m_{\tilde{q}}$ (GeV)	$m_{\tilde{g}}$ (GeV)	σ (pb)
B1	100.1	$\tilde{\tau}$	577	631	42
B2	100.4	$\tilde{\ell}$	563	617	50
B3	101.0	$\tilde{\tau}$	1190	1480	0.59
B4	103.4	$\tilde{\ell}$	721	859	10
B5	251.2	$\tilde{\tau}$	1910	2370	0.023
B6	245.3	$\tilde{\ell}$	1290	1410	0.36
B7	399.2	$\tilde{\tau}$	2000	2170	0.017
B8	302.9	$\tilde{\ell}$	1960	2430	0.022

Table 3: *Features of the sample GMSB model points studied.*

detailed response of the detector to the slepton NLSP has been parametrised for this work using the results of a full simulation study, as described in the next section.

B.3 Slepton detection

The experimental signatures of heavy long-lived charged particles at a hadron collider have already been studied both in the framework of GMSB and in more general scenarios [35–38]. The two main observables one can use to separate these particles from muons are the high specific ionisation and the time of flight in the detector.

We concentrate here on the measurement of the time of flight, made possible by the timing precision ($\lesssim 1$ ns) and the size of the ATLAS muon spectrometer.

It was demonstrated with a full simulation of the ATLAS muon detector [39] that the β of a particle can be measured with a resolution that can be approximately parameterised as $\sigma(\beta)/\beta^2 = 0.028$. The resolution on the transverse momentum measurement for heavy particles is found to be comparable to the one expected for muons. We have therefore simulated the detector response to NLSP sleptons by smearing the slepton momentum and β according to the parameterisations in Ref. [39].

An important issue is the online selection of the SUSY events. We have not made any attempt to evaluate whether the heavy sleptons can be selected using the muon trigger. For the event selection, we rely on the calorimetric $E_T^{\rm miss}$ trigger, consisting in the requirement of at least a hadronic jet with $p_T > 50$ GeV, and a transverse momentum imbalance calculated only from the energy deposition in the calorimeter larger than 50 GeV. We checked that this trigger has an efficiency in excess of 80% for all the considered models.

A detailed discussion of the experimental assumptions underlying the results presented here is given in Ref. [40].

B.4 Event Selection and Slepton Mass Measurement

In order to select a clean sample of sleptons, we apply the following requirements:

- at least a hadronic jet with $P_T > 50$ GeV and a calorimetric $E_T^{\rm miss} > 50$ GeV (trigger requirement);
- at least one candidate slepton satisfying the following cuts:

- $|\eta|$ <2.4 to ensure that the particle is in the acceptance of the muon trigger chamber, and therefore both coordinates can be measured;
- $\beta_{\rm meas} < 0.91$, where $\beta_{\rm meas}$ is the β of the particle measured with the time of flight in the precision chambers;
- The P_T of the slepton candidate, after the energy loss in the calorimeters has been taken into account, must be larger than 10 GeV, to ensure that the particle traverse all of the muon stations.

Considering an integrated luminosity of 30 fb^{-1}, a number of events ranging from a few hundred for the models with 2 TeV squark mass scale to a few hundred thousand for a 500 GeV mass scale survive these cuts and can be used for measuring the NLSP properties.

From the measurements of the slepton momentum and of particle β, the mass can be determined using the standard relation $m = p\frac{\sqrt{1-\beta^2}}{\beta}$. For each value of β and momentum, the measurement error is known and it is given by the parametrisations in Ref. [39]. Therefore, the most straightforward way of measuring the mass is just to use the weighted average of all the masses calculated with the above formula.

In order to perform this calculation, the particle momentum is needed, which implies measuring the η coordinate. In fact, with the precision chambers only one can only measure the momentum components transverse to the beam axis.

The measurement of the second coordinate must be provided by the trigger chambers, for which only a limited time window around the beam crossing is read out, therefore restricting the β range where this measurement is available. Hence, we have evaluated the achieved measurement precision for two different β intervals: $0.6 < \beta < 0.91$ and $0.8 < \beta < 0.91$ for the eight sample points. We found a statistical error well below the 0.1% level for those model points having $m_{\tilde{q}} < 1300$ GeV. Even for the three models (B5, B7, B8) with lower statistics ($m_{\tilde{q}} \simeq 2$ TeV), the error stays below the 0.4% level.

Many more details, tables and figures about this part of our study can be found in Ref. [40].

B.5 Slepton Lifetime Measurement

The measurement of the NLSP lifetime at a high energy e^+e^- collider was studied in detail in Ref. [8] for the neutralino NLSP case. Similar to that study, the measurement of the slepton NLSP lifetime we are interested in here can be performed by exploiting the fact that two NLSP's are produced in each event. One can therefore select N_1 events where a slepton is detected through the time-of-flight measurement described above, count the number of times N_2 when a second slepton is observed and use this information to measure the lifetime. Although in principle very simple, in practice this method requires an excellent control on all possible sources of inefficiency for detecting the second slepton.

We give here the basis of the method, without mentioning the experimental details. We provide an estimate of the achievable statistical error for the models considered and a parametrisation of the effect on the lifetime measurement of a generic systematic uncertainty on the slepton efficiency. In case the sparticle spectrum and BR's can be measured from the SUSY events, as e.g. shown in Ref. [41], an accurate simulation of all the SUSY production processes can be performed, and the results from this section are representative of the measurement precision achievable in a real experiment.

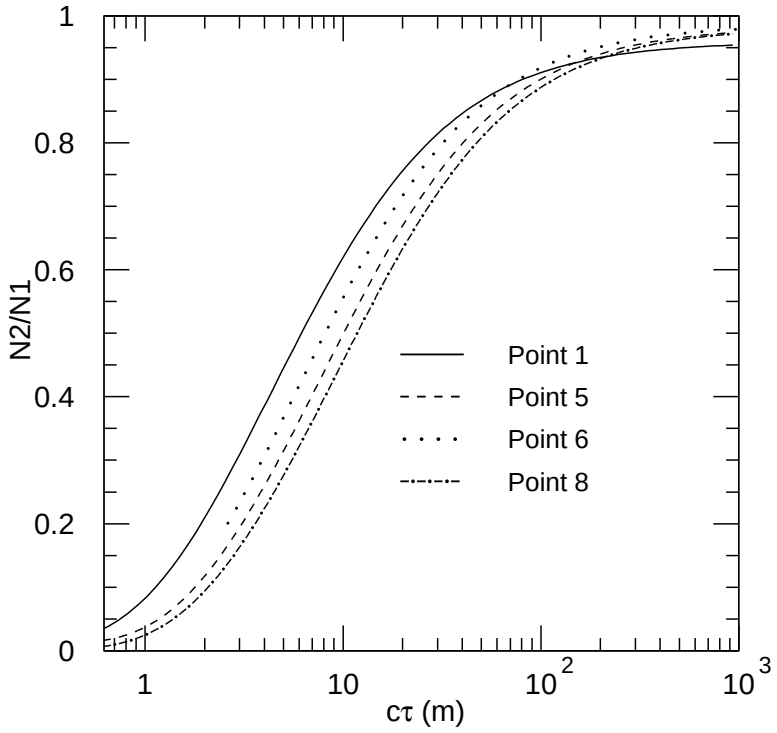

Figure 5: *The ratio $R = N_2/N_1$ defined in the text as a function of the slepton lifetime $c\tau$. Only the curves corresponding to the model points B1, B5, B6, B8 are shown.*

Another method based on the same principles, but assuming minimal knowledge of the SUSY spectrum, is described in Ref. [40], where a detailed estimate of the achievable systematic precision is given.

We define N_1 starting from the event sample defined by the cuts discussed in Sec. 1, with the additional requirement that, for a given value of the slepton lifetime, at least one of the produced sleptons decays at at a distance from the interaction vertex > 10 m, and is therefore reconstructed in the muon system. For the events thus selected, we define N_2 as the subsample where a second particle with a transverse momentum > 10 GeV is identified in the muon system. The search for the second particle should be as inclusive as possible, in order to minimise the corrections to the ratio. In particular, the cut $\beta_{\rm meas} < 0.91$ is not applied, but particles with a mass measured from β and momentum incompatible with the measured slepton mass are rejected. This leaves a background of high momentum muons in the sample that can be statistically subtracted using the momentum distribution of electrons. The ratio

$$R = \frac{N_2}{N_1} \tag{7}$$

is a function of the slepton lifetime. Its dependence on the NLSP lifetime $c\tau$ in metres in shown in Fig. 5 for four among our eight sample models. The curves for the model points not shown are either very similar to one of the curves we show or are mostly included between the external curves corresponding to points B1 and B8, thus providing no essential additional information. Note that the curve for model 6 starts from $c\tau = 2.5$ m and not from $c\tau = 50$ cm, as for the other models. This is due to the large value of $M_{\rm mess}$ (cfr.

Tab. 2), determining a minimum NLSP lifetime allowed by theory which is macroscopic in this case [cfr. Eqs. (3) and (5)].

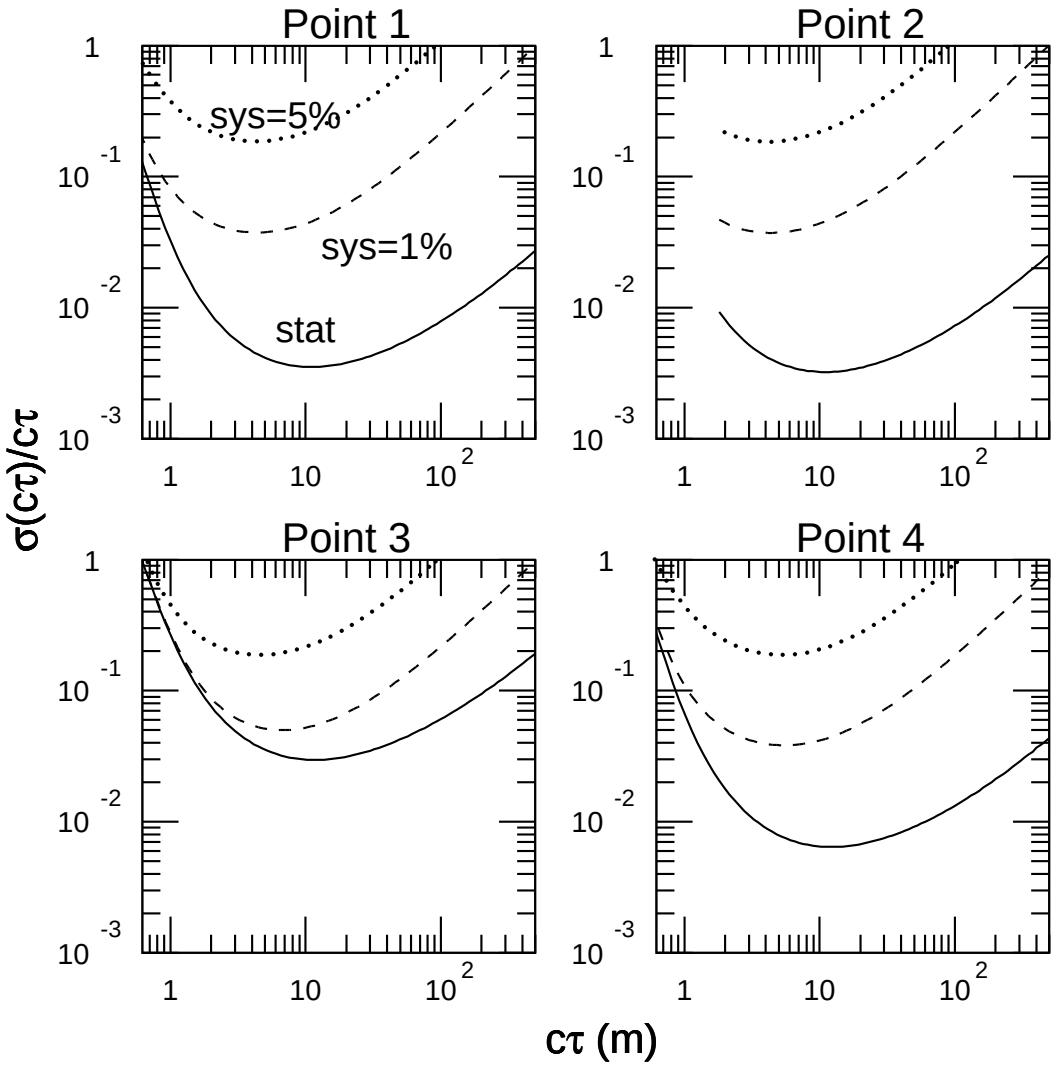

Figure 6: *Fractional error on the measurement of the slepton lifetime $c\tau$, for model sample points B1 to B4. We assume an integrated luminosity of 30 fb^{-1}. The curves are shown for three different assumptions on the fractional systematic error on the R measurement: statistical error only (full line), 1% systematic error (dashed line), 5% systematic error (dotted line).*

The probability for a particle of mass m, momentum p and proper lifetime τ to travel a distance L before decaying is given by the expression

$$P(L) = e^{-mL/pc\tau}. \tag{8}$$

N_2 is therefore a function of the momentum distribution of the slepton, which is determined by the details of the SUSY spectrum. One needs therefore to be able to simulate the full SUSY cascade decays in order to construct the $c\tau$–R relationship.

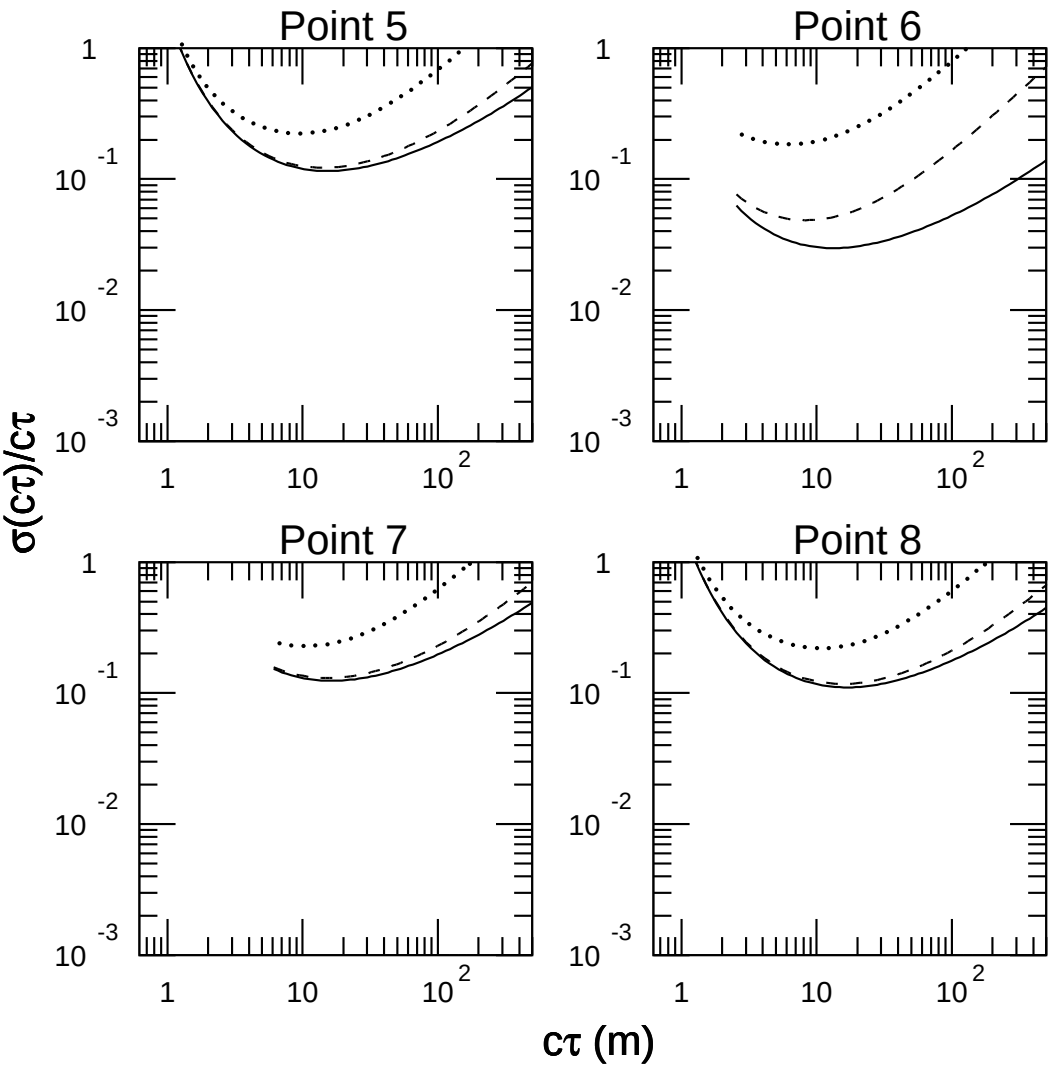

Figure 7: *The same as in Fig. 7, but for the model sample points B5 to B8.*

The statistical error on R can be evaluated as

$$\sigma(R) = \sqrt{\frac{R(1-R)}{N_1}}. \tag{9}$$

Relevant for the precision with which the SUSY breaking scale can be measured is instead the error on the measured $c\tau$. This can be extracted from the curves shown in Fig. 5 and can be evaluated as

$$\sigma(\mathrm{c}\tau) = \sigma(R) / \left[\frac{\partial R(c\tau)}{\partial c\tau}\right]. \tag{10}$$

The measurement precision calculated according to this formula is shown in Figs. 6 and 7 for the eight sample points, for an integrated luminosity of 30 fb^{-1}. The full line in the plots is the error on $c\tau$ considering the statistical error on R only. The available statistics is a function of the strongly interacting sparticles' mass scale. Even if a precise R–$c\tau$

relation can be built from the knowledge of the model details, there will be a systematic uncertainty in the evaluation of the losses in N_2, because of sleptons produced outside the η acceptance, or absorbed in the calorimeters, or escaping the calorimeter with a transverse momentum below the cuts. The full study of these uncertainties is in progress.

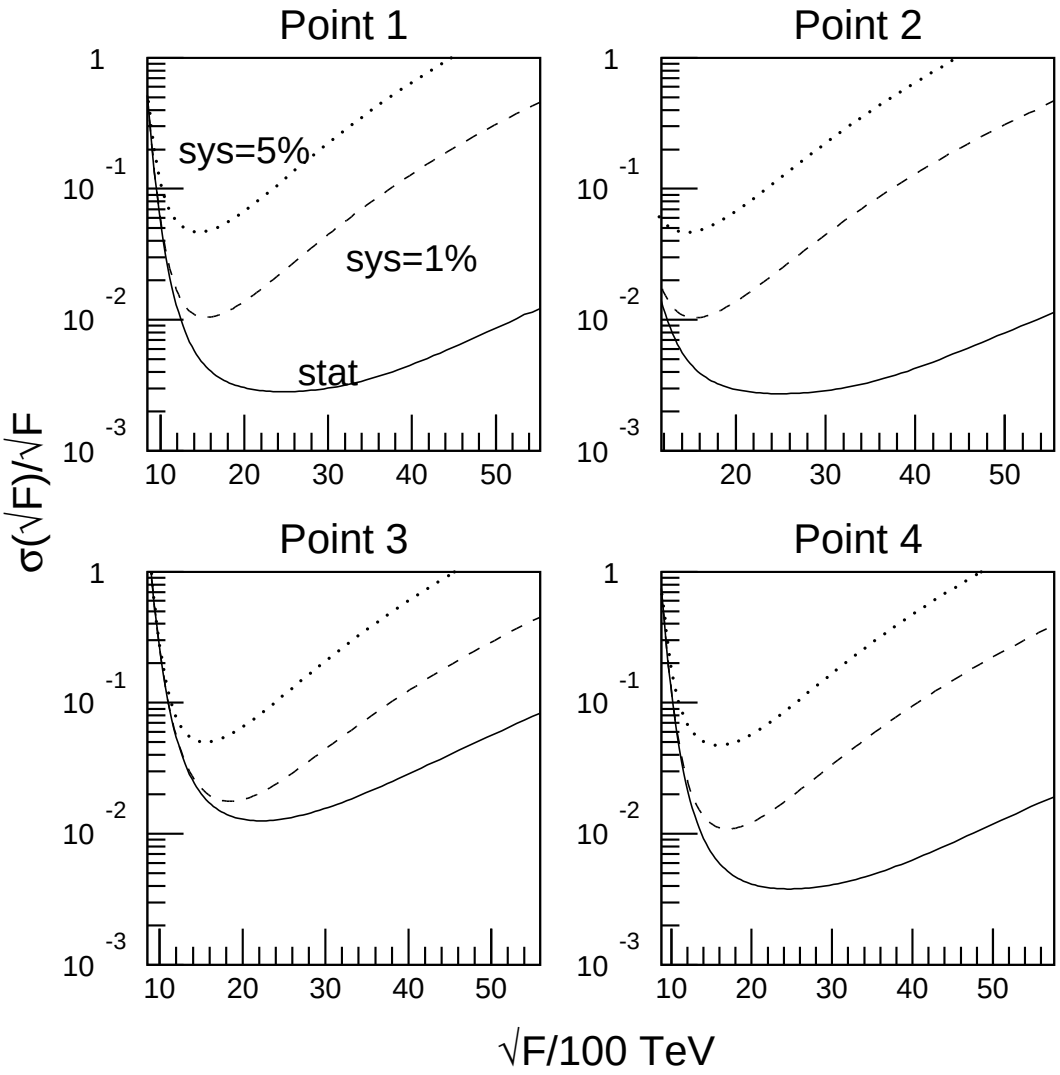

Figure 8: *Fractional error on the measurement of the SUSY breaking scale $\sqrt{F}$ for model sample points B1 to B4. We assume an integrated luminosity of 30 fb^{-1}. The curves are shown for the three different assumptions on the fractional systematic error used in Figs. 6 and 7.*

At this level, we just parameterise the systematic error as a term proportional to R, added in quadrature to the statistical error. We choose two values, 1%R and 5%R, and propagate the error to the $c\tau$ measurement. The results are represented by the dashed and dotted lines in Figs. 6 and 7.

For the models with squark mass scales up to 1200 GeV, assuming a 1% systematic error on the measured ratio, a precision better than 10% on the $c\tau$ measurement can be obtained for lifetimes between 0.5–1 m and 50–80 m. If the systematic uncertainty grows

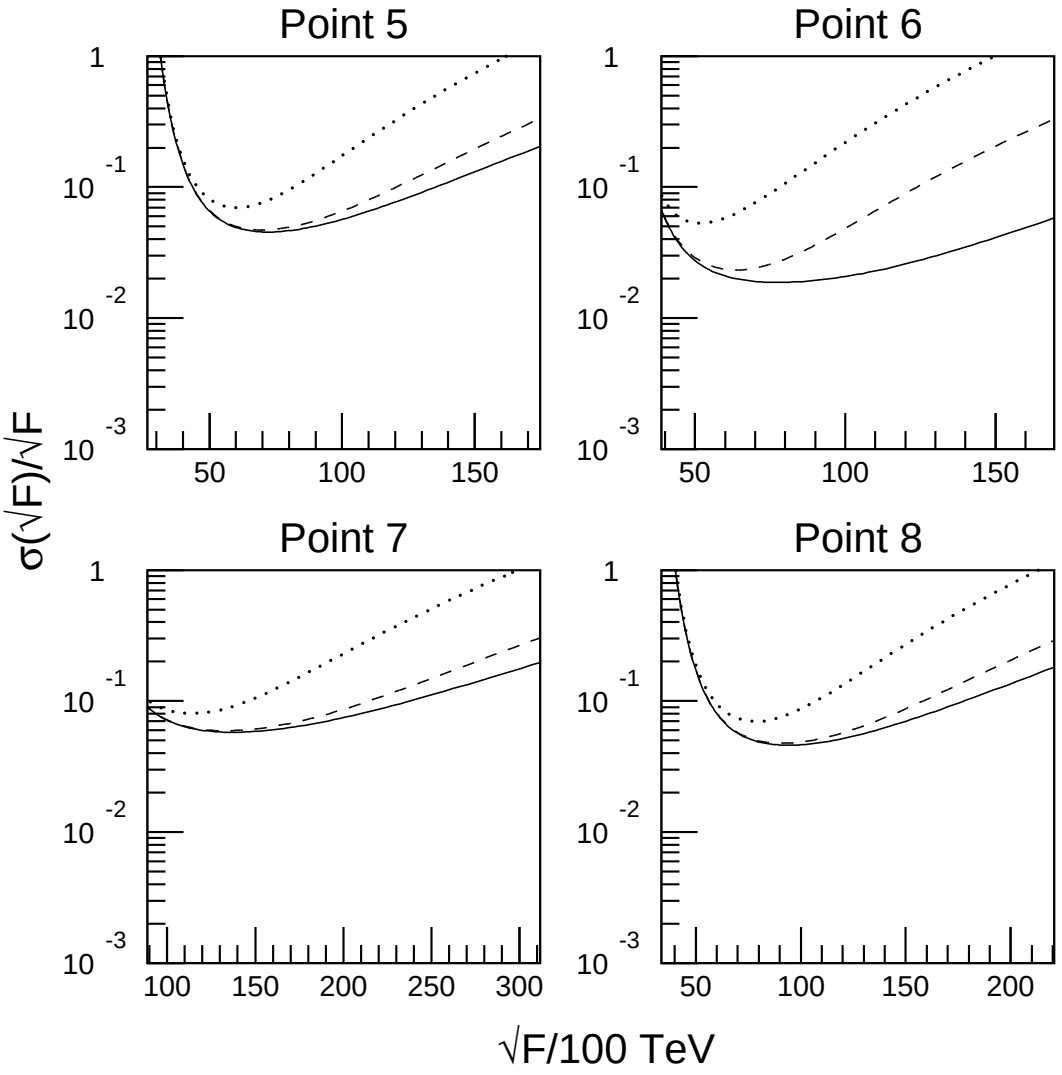

Figure 9: *The same as in Fig. 8, but for model sample points B5 to B8.*

to 5%, the 10% precision can only be achieved in the range 1–10 m. If the mass scale goes up to 2 TeV, even considering a pure statistical error only, a 10% precision is not achievable. However a 20% precision is possible over $c\tau$ ranges between 5 and 100 m, assuming a 1% systematic error.

Note that the curves corresponding to the model points B2, B6 and B7 do not start from $c\tau = 50$ cm, but from the theoretical lower limit on $c\tau$ of 1.8, 2.5 and 6.1 metres, respectively.

B.6 Determining the SUSY Breaking Scale $\sqrt{F}$

Using the measured values of $c\tau$ and the NLSP mass, the SUSY breaking scale $\sqrt{F}$ can be calculated from Eq. (3), where $\mathcal{B} = 1$ for the case where the NLSP is a slepton. From simple error propagation, the fractional uncertainty on the $\sqrt{F}$ measurement can be obtained adding in quadrature one fourth of the fractional error in $c\tau$ and five fourths

of the fractional error on the slepton mass.

In Figs. 8 and 9, we show the fractional error on the $\sqrt{F}$ measurement as a function of $\sqrt{F}$ for our three different assumptions on the $c\tau$ error. The uncertainty is dominated by $c\tau$ for the higher part of the $\sqrt{F}$ range and grows quickly when approaching the lower limit on $\sqrt{F}$. This is because very few sleptons survive and the statistical error on both $m_{\tilde{\ell}}$ and $c\tau$ gets very large. If we assume a 1% systematic error on the ratio R from which $c\tau$ is measured (dashed lines in Figs. 8 and 9), the error on $\sqrt{F}$ is better than 10% for $1000 \lesssim \sqrt{F} \lesssim 4000$ TeV for model points B1–B4 with higher statistics. For points B5–B8, in general one can explore a range of higher $\sqrt{F}$ values with a small relative error, essentially due to the heaviness of the decaying NLSP in these models. Note also that the theoretical lower limit (5) on $\sqrt{F}$ is equal to about 1200, 1500, 3900, 8900 TeV respectively in model points B2, B5, B6, B7, while it stays well below 1000 TeV for the other models.

B.7 Conclusions

We have discussed a simple method to measure at the LHC with the ATLAS detector the fundamental SUSY breaking scale $\sqrt{F}$ in the GMSB scenarios where a slepton is the NLSP and decays to the gravitino with a lifetime in the range 0.5 m $\lesssim c\tau_{\rm NLSP} \lesssim$ 1 km. This method requires the measurement of the time of flight of long lived sleptons and is based on counting events with one or two identified NLSP's. It relies on the assumptions that a good knowledge of the MSSM sparticle spectrum and BR's can be extracted from the observation of the SUSY events and that the systematic error in evaluating the slepton losses can be kept below the few percent level. We performed detailed, particle level simulations for eight representative GMSB models, some of them being particularly hard due to low statistics. We found that a level of precision of a few 10's % on the SUSY breaking scale measurement can be achieved in significant parts of the $1000 \lesssim \sqrt{F} \lesssim 30000$ TeV range, for all models considered. More details as well as a full study of the systematics associated with this procedure and another less "model-dependent" method to measure $\sqrt{F}$ is presented in detail in Ref. [40].

Acknowledgements

S. A. and G. P. thank the organisers of the Workshop "Physics at TeV Colliders", for the hospitality and the pleasant and productive atmosphere in Les Houches.

References

[1] For a recent pedagogical review of supersymmetry and supersymmetry breaking, see S. P. Martin, "A Supersymmetry Primer", in "Perspectives on Supersymmetry", G. L. Kane ed., World Scientific 1998, hep-ph/9709356 and references therein.

[2] M. Dine, W. Fischler, M. Srednicki, Nucl. Phys. **B189** (1981) 575; S. Dimopoulos, S. Raby, Nucl. Phys. **B192** (1981) 353; M. Dine, W. Fischler, Phys. Lett. **110B** (1982) 227; M. Dine, M. Srednicki, Nucl. Phys. **B202** (1982) 238; M. Dine, W. Fischler, Nucl. Phys. **B204** (1982) 346; L. Alvarez-Gaumé, M. Claudson, M. B. Wise,

Nucl. Phys. **B207** (1982) 96; C. R. Nappi, B. A. Ovrut, Phys. Lett. **113B** (1982) 175; S. Dimopoulos, S. Raby, Nucl. Phys. **B219** (1983) 479.

[3] M. Dine, A. E. Nelson, Phys. Rev. D **48** (1993) 1277; M. Dine, A. E. Nelson, Y. Shirman, Phys. Rev. D **51** (1995) 1362; M. Dine, A. E. Nelson, Y. Nir, Y. Shirman, Phys. Rev. D **53** (1996) 2658.

[4] For a recent review, see G. F. Giudice, R. Rattazzi, "Theories with Gauge-Mediated Supersymmetry Breaking", hep-ph/9801271, submitted to Phys. Rep.

[5] S. Dimopoulos, S. Thomas, J. D. Wells, Phys. Rev. D **54** (1996) 3283; Nucl. Phys. **B488** (1997) 39.

[6] J. A. Bagger, K. Matchev, D. M. Pierce, R. Zhang, Phys. Rev. D **55** (1997) 3188.

[7] S. Ambrosanio, G. D. Kribs, S. P. Martin, Phys. Rev. D **56** (1997) 1761.

[8] S. Ambrosanio, G. A. Blair, Eur. Phys. J. C **12** (2000) 287–321.

[9] P. Fayet, Phys. Lett. **70B** (1977) 461; Phys. Lett. **86B** (1979) 272; Phys. Lett. B **175** (1986) 471 and in "Unification of the fundamental particle interactions", eds. S. Ferrara, J. Ellis, P. van Nieuwenhuizen (Plenum, New York, 1980) p. 587.

[10] A relevant example is discussed in: S. Ambrosanio, G. D. Kribs, S. P. Martin, Nucl. Phys. **B516** (1998) 55.

[11] An updated, generalised and `Fortran`-linked version of the program used in Ref. [7]. It generates minimal and non-minimal GMSB and SUGRA models. For inquiries about this software package, please send e-mail to `ambros@mail.cern.ch`.

[12] S. Ambrosanio, S. Heinemeyer, G. Weiglein, in preparation.

[13] A. Dedes, S. Heinemeyer, P. Teixeira-Dias, G. Weiglein, hep-ph/9912249, to appear in Jour. Phys. G.

[14] H. Haber, R. Hempfling, Phys. Rev. Lett. **66** (1991) 1815; J. Ellis, G. Ridolfi, F. Zwirner, Phys. Lett. B **257** (1991) 83; Phys. Lett. B **262** (1991) 477.

[15] P. Chankowski, S. Pokorski, J. Rosiek, Nucl. Phys. **B423** (1994) 437.

[16] A. Dabelstein, Nucl. Phys. **B456** (1995) 25; Z. Phys. C **67** (1995) 495.

[17] J. Bagger, K. Matchev, D. Pierce, R. Zhang, Nucl. Phys. **B491** (1997) 3.

[18] J. Casas, J. Espinosa, M. Quirós, A. Riotto, Nucl. Phys. **B436** (1995) 3, E: ibid **B439** (1995) 466; M. Carena, J. Espinosa, M. Quirós, C. Wagner, Phys. Lett. B **355** (1995) 209; M. Carena, M. Quirós, C. Wagner, Nucl. Phys. **B461** (1996) 407.

[19] H. Haber, R. Hempfling, A. Hoang, Z. Phys. C **75** (1997) 539.

[20] R. Hempfling, A. Hoang, Phys. Lett. B **331** (1994) 99; R.-J. Zhang, Phys. Lett. B **447** (1999) 89.

[21] S. Heinemeyer, W. Hollik, G. Weiglein, Phys. Rev. D **58** (1998) 091701; Phys. Lett. B **440** (1998) 296.

[22] S. Heinemeyer, W. Hollik, G. Weiglein, Eur. Phys. J. C **9** (1999) 343.

[23] S. Heinemeyer, W. Hollik, G. Weiglein, Phys. Lett. B **455** (1999) 179.

[24] P. McNamara, "Combined LEP Higgs search results up to $\sqrt{s} = 196$ GeV", talk given at the LEPC meeting, September 7, 1999.

[25] S. Heinemeyer, W. Hollik, G. Weiglein, Comp. Phys. Comm. **124** (2000) 76.

[26] S. Heinemeyer, W. Hollik, G. Weiglein, hep-ph/9910283.

[27] M. Carena, H. Haber, S. Heinemeyer, W. Hollik, C. Wagner, G. Weiglein, DESY 197-99, hep-ph/0001002.

[28] T. A. Kaeding, S. Nandi, hep-ph/9906432.

[29] See e.g.: H. Pagels, J. R. Primack, Phys. Rev. Lett. **48** (1982) 223.

[30] S. Heinemeyer, W. Hollik, G. Weiglein, hep-ph/9909540.

[31] M. Carena, S. Heinemeyer, C. Wagner, G. Weiglein, hep-ph/9912223.

[32] The ATLAS Collaboration, "ATLAS Detector and Physics Performance Technical Design Report", ATLAS TDR 15, CERN/LHCC/99-15 (1999).

[33] H. Baer, F. E. Paige, S. D. Protopopescu, X. Tata, hep-ph/9305342; hep-ph/9804321.

[34] E. Richter-Was, D. Froidevaux, L. Poggioli, "`ATLFAST 2.0`: A Fast Simulation Package for ATLAS", ATLAS Internal Note ATL-PHYS-98-131 (1998).

[35] A. Nisati, S. Petrarca, G. Salvini, Mod. Phys. Lett. **A12** (1997) 2213.

[36] M. Drees, X. Tata, Phys. Lett. B **252** (1990) 695.

[37] J. L. Feng, T. Moroi, Phys. Rev. D **58** (1998) 035001.

[38] S. P. Martin, J. D. Wells, Phys. Rev. D **59** (1999) 035008.

[39] G. Polesello, A. Rimoldi, "Reconstruction of Quasi-stable Charged Sleptons in the ATLAS Muon Spectrometer", ATLAS Internal Note ATL-MUON-99-06.

[40] S. Ambrosanio, B. Mele, S. Petrarca, G. Polesello, A. Rimodi, in preparation.

[41] I. Hinchliffe, F. E. Paige, Phys. Rev. D **60** (1999) 095002.